JOURNAL OF VIROLOGY, Apr. 2008, p. 3369–3380 Vol. 82, No. 7
0022-538X/08/$08.00+0 doi:10.1128/JVI.02243-07

Human HLA-DR Transgenes Protect Mice from Fatal Virus-Induced Encephalomyelitis and Chronic Demyelination▽

Moses Rodriguez,[1,2]* Laurie Zoecklein,[1] Jason G. Kerkvliet,[1] Kevin D. Pavelko,[1] Louisa Papke,[1] Charles L. Howe,[2] Larry R. Pease,[2] and Chella David[2]

Departments of Immunology[1] and Neurology,[2] Mayo Clinic, Rochester, Minnesota 55905

Received 16 October 2007/Accepted 16 January 2008

We evaluated the participatory role of human HLA-DR molecules in control of virus from the central nervous system and in the development of subsequent spinal cord demyelination. The experiments utilized intracranial infection with Theiler's murine encephalomyelitis virus (TMEV), a picornavirus that, in some strains of mice, results in primary demyelination. We studied DR2 and DR3 transgenic mice that were bred onto a combined class I-deficient mouse (beta-2 microglobulin deficient; $\beta2m^0$) and class II-deficient mouse ($A\beta^0$) of the *H-2*^{b} background. $A\beta^0.\beta2m^0$ mice infected with TMEV died within 18 days of infection. These mice showed severe encephalomyelitis due to rapid replication of virus genome. In contrast, transgenic mice with insertion of a single human class II major histocompatibility complex (MHC) gene (DR2 or DR3) survived the acute infection. DR2 and DR3 mice controlled virus infection by 45 days and did not develop spinal cord demyelination. Levels of virus RNA were reduced in HLA-DR transgenic mice compared to $A\beta^0.\beta2m^0$ mice. Virus-neutralizing antibody responses did not explain why DR mice survived the infection and controlled virus replication. However, DR mice showed an increase in gamma interferon and interleukin-2 transcripts in the brain, which were associated with protection. The findings support the hypothesis that the expression of a single human class II MHC molecule can, by itself, influence the control of an intracerebral pathogen in a host without a competent class I MHC immune response. The mechanism of protection appears to be the result of cytokines released by $CD4^+$ T cells.

An important question in neurovirology and neuroimmunology is how virus infections are controlled in the central nervous system. This question is particularly important when viruses persist in the brain or spinal cord but are cleared from the tissues outside the central nervous system (CNS). There is evidence that specific aspects of the immune system clear specific classes of viruses. For example, antibody may be critically important for virus control in the CNS in certain arbovirus infections (9). In contrast, arenaviruses, such as lymphocytic choriomeningitis virus, require class I-restricted cytotoxic lymphocytes to eliminate intracerebral infection (50). Cytotoxicity may not be necessary for virus control by lymphocytes. Instead, the factors secreted by cells in the inflammatory infiltrate may control virus infection in neurons and other CNS cells. Gamma interferon (IFN-γ) has been shown in several model systems to be essential for virus control in the CNS (27, 46, 48). Other cytokines such as interleukin-6 (IL-6) may also help protect neurons from virus injury (35). Natural killer cells have also been shown to be critical in preventing fulminant virus-induced encephalitis (37).

Most of the investigative work on controlling CNS virus infection has been done in rodents. Little data exist about the human immune factors contributing to this process. In an attempt to approach this difficult problem, we created a series of human HLA transgenic mice. We originally created class II $A\beta^0$ mice without endogenous $CD4^+$ T-cell-dependent immune responses. We then substituted the human class II gene (DR2 or DR3) for the mouse class II response. These mice mount normal class II-restricted CD4 T-cell-mediated immune responses to a number of antigens and infectious agents, (5, 14, 23, 34) and have an intact mouse $CD8^+$ T-cell-restricted endogenous class I major histocompatibility complex (MHC) immune response. Therefore, we could not exclude the contribution of the endogenous mouse MHC class I response to antigen challenge. We mated the $A\beta^0$.DR transgenic mice to beta-2 microglobulin-deficient mice ($\beta2m^0$) and generated lines of mice deficient in both the mouse endogenous class I and class II immune responses. Thus, responses observed in these mice would be uniquely the consequence of the human class II gene.

We tested these mice with a naturally occurring viral pathogen of the CNS. Our laboratory has investigated virus control, virus persistence, and demyelination following intracerebral injection of Theiler's murine encephalomyelitis virus (TMEV), a picornavirus that induces a characteristic biphasic disease in the CNS of immune competent mice (3, 21). During the first 10 to 12 days of infection, the virus replicates primarily in neurons of the hippocampus, striatum, cortex of the brain, and anterior horn cells of the spinal cord and then clears rapidly from these cells irrespective of MHC haplotype. Oligodendrocytes and macrophages are also infected early (31). In mice that control virus infection (MHC haplotype *H-2*^{b,d,k}), no virus antigen persistence develops and therefore no spinal cord demyelination ensues (41). In mice that do not control virus infection (MHC haplotype *H-2*^{s,v,r,u,f}), virus antigen persists in glial cells (45) and macrophages (2, 15, 49), in particular in the spinal cord white matter and brain stem. This results in primary

* Corresponding author. Mailing address: Departments of Neurology, Mayo Clinic, 200 First St. SW, Rochester, MN 55905. Phone: (507) 284-4663. Fax: (507) 284-1087. E-mail: rodriguez.moses@mayo.edu.

▽ Published ahead of print on 30 January 2008.

demyelination, inflammation, axonal loss, and neurologic deficits similar to human multiple sclerosis.

We infected $A\beta^0.\beta2m^0$.DR2 and $A\beta^0.\beta2m^0$.DR3 mice with TMEV and examined them for survival, neuropathology, virus replication, and cytokine expression in the brain. Our controls were $A\beta^0.\beta2m^0$, $A\beta^0$, $\beta2m^0$, and B6 mice. All of the experimental mice were of the *H-2*^{b} haplotype that controls virus infection (41). As a positive control mouse that develops virus antigen persistence and demyelination, we used B10.Q and SJL mice of the *H-2*^{q} and *H-2*^{s} haplotypes.

MATERIALS AND METHODS

Virus. We used Daniel's strain of TMEV for all experiments (21).

Mice. All mice were generated in the Mayo Clinic College of Medicine Transgenic Core Facility under the direction of Chella David. We crossed $A\beta^0$.DR2 and $A\beta^0$.DR3 to $\beta2m^0$ mice to generate lines of $A\beta^0.\beta2m^0$.DR2 and $A\beta^0.\beta2m^0$.DR3 mice. We used $A\beta^0.\beta2m^0$, and C57BL/6 (black) mice as controls. Littermate controls for these mice are described in the text. For a positive control mouse strain that develops chronic demyelination, we used B10.Q *H-2*^{q} mice. We chose this strain as a positive control because it shares the same C57BL (black) background as the other mice in the experiment. Experiments were approved by the Mayo IACUC and conformed to guidelines for the care of animals by the National Institutes of Health. Mice were followed daily until they were moribund or died. Mice that survived the acute infection were sacrificed on day 45 (endpoint of the study) after infection for pathology and virus RNA expression. Some of the data include $A\beta^0.\beta2m^0$.DR4 mice. However, the data on these mice are limited because they were difficult to breed.

Infection and harvesting of the CNS for morphology. At 4 to 6 weeks of age, mice were intracerebrally infected with 2×10^5 PFU of TMEV in a total volume of 10 μl. At various times after infection, mice were perfused via intracardiac puncture with 50 ml of Trump's fixative. Spinal cords and brains were removed and postfixed for 24 to 48 h in Trump's fixative in preparation for morphological analysis.

Spinal cord morphometry. Spinal cords were cut into 1-mm coronal blocks. Every third block was osmicated and embedded in glycol methacrylate. Two-micrometer sections were prepared and stained with a modified erichrome/cresyl violet stain (38). Morphological analysis was performed on 12 to 15 sections per mouse as previously described (43). Each quadrant from every coronal section from each mouse was graded for the presence or absence of gray matter disease, meningeal inflammation, and demyelination. The score was expressed as the percentage of spinal cord quadrants examined with the pathological abnormality. A maximum score of 100 indicated a particular pathological abnormality in every quadrant of all spinal cord sections of a given mouse. All grading was performed without knowledge of the experimental group. Additional spinal cord blocks were embedded in paraffin for immunocytochemistry.

Brain pathology. Brain pathology was assessed at days 18 and 45 postinfection, using our previously described technique (35). Following perfusion with Trump's fixative, we made two coronal cuts in the intact brain at the time of removal from the skull (one section through the optic chiasm and a second section through the infundibulum). As a guide, we used the *Atlas of the Mouse Brain and Spinal Cord* corresponding to sections 220 and 350, page 6 (51). This resulted in three blocks that were then embedded in paraffin. This allowed for systematic analysis of the pathology of the cortex, corpus callosum, hippocampus, brain stem, striatum, and cerebellum. The resulting slides were then stained with hematoxylin and eosin. Pathological scores were assigned without knowledge of experimental group to the following areas of the brain: cortex, corpus callosum, hippocampus, brainstem, striatum, and cerebellum. Each area of the brain was graded on a four-point scale as follows: 0, no pathology; 1, no tissue destruction but only minimal inflammation; 2, early tissue destruction (loss of architecture) and moderate inflammation; 3, definite tissue destruction (demyelination, parenchymal damage, cell death, neurophagia, neuronal vacuolation); and 4, necrosis (complete loss of all tissue elements with associated cellular debris). Meningeal inflammation was assessed and graded as follows: 0, no inflammation; 1, one cell layer of inflammation; 2, two cell layers of inflammation; 3, three cell layers of inflammation; 4, four or more cell layers of inflammation. The area with the maximal extent of tissue damage was used for assessment of each brain region.

Immune staining for virus antigen. Immunocytochemistry was performed on paraffin-embedded sections as previously described (35). Slides were deparaffinized in xylene and rehydrated through an ethanol series (absolute, 95%, 70%, and 50%). Virus antigen staining was carried out using polyclonal antisera to TMEV DA (45), which reacts strongly with the capsid proteins of TMEV. Following incubation with a secondary biotinylated antibody (Vector Laboratories, Burlingame, CA), immunoreactivity was detected using the avidin-biotin immunoperoxidase technique (Vector Laboratories). The reaction was developed using Hanker-Yates reagent with hydrogen peroxide as the substrate (Polysciences, Warrington, PA). Slides were lightly counterstained with Mayer's hematoxylin. We examined the distribution of virus antigen in the spinal cords of B6, $\beta2m^0$, $A\beta^0$, $A\beta^0.\beta2m^0$, $A\beta^0.\beta2m^0$.DR2, and $A\beta^0.\beta2m^0$.DR3 mice at 18 and 45 days after infection. For this analysis, we scored every spinal quadrant for the presence or absence of virus antigen-positive cells in either the gray matter or white matter in every animal. Five randomly selected mice were included in each group. We examined on average 10 spinal cord sections with representative samples from the cervical, thoracic, and lumbar areas. The data were expressed as the percentage of spinal cord quadrants showing virus antigen-positive cells in either the gray matter or white matter of the spinal cord.

RNA isolation. We removed the brain and spinal cords from animals infected with TMEV. Total RNA was extracted from brain and spinal cord (48). Briefly, the tissues were frozen and stored in liquid nitrogen. Tissue samples were homogenized in the RNA STAT-60 (1 ml/100 mg tissue) (Tel-Test, Inc., Friendswood, TX), and total RNA was isolated according to the manufacturer's recommendations. The RNA concentrations were determined by spectrophotometer. The RNA samples were equilibrated to a concentration of 0.25 μg/μl and stored at −80°C.

RT-PCR and real-time analysis for virus RNA. We used the VP2 fragment of TMEV, a viral capsid region of DA virus, for reverse transcription-PCR (RT-PCR) (48). The primer pair sequences for VP2 of DA virus were as follows: 5′-TGGTCGACTCTGTGGTTACG-3′ (forward) and 5′-GCCGGTCTTGCAA AGATAGT-3′ (reverse). Glyceraldehyde-3-phosphate dehydrogenase (GAPDH) was used as a control for intersample variability. The sequences used for assaying the presence of GAPDH were as follows: 5′-ACCACCATGGAGAAGGC-3′ (forward) and 5′-GGCATGGACTGTGGTCATGA-3′ (reverse). The sizes of PCR products amplified with primers were 238 bp for VP2 and 236 bp for GAPDH.

Standards were generated by serial 10-fold dilutions of plasmid cDNA. Standards were amplified in parallel with unknown samples by real-time quantitative RT-PCR using the LightCycler (Roche, Indianapolis, IN) as per the manufacturer's instructions.

Quantification of cytokine RNA from the brain by real-time RT-PCR. The primer sequences for each gene were as follows: GAPDH forward, 5′-AGCTT GTCATCAACGGGAAG-3′, and reverse, 5′-TTTGATGTTAGTGGGGTCTC G-3′; IL-2 forward, 5′-GCTGTTGATGGACCTACAGGA-3′, and reverse, 5′-ATCCTGGGGAGTTTCAGGTT-3′; IL-4 forward, 5′-CATCGGCATTTTGA ACGAG-3′, and reverse, 5′-ACGTTTGGCACATCCATCTC-3′; IL-6 forward, 5′-GCTACCAAACTGGATATAATCAGGA-3′, and reverse, 5′-CCAGGTAG CTATGGTACTCCAGAA-3′; IL-10 forward, 5′-ACTGCACCCACTTCCCAG T-3′, and reverse, 5′-TGTCCAGCTGGTCCTTTGTT-3′; IFN-γ forward, 5′-T CTGGAGGAACTGGCAAAAG-3′, and reverse, 5′-TTCAAGACTTCAAAG AGTCTGAGG-3′; and tumor necrosis factor (TNF), forward, 5′-CTGTAGCC CACGTCGTAGC-3′, and reverse, 5′-TTGAGATCCATGCCGTTG-3′. Percent expression relative to control GAPDH was calculated using the equation: % expression = {[1.9^(average crossing point of experimental gene for control group − crossing point of experimental gene for each sample)]/[1.9^(average crossing point of GAPDH in the control group − crossing point of GAPDH for each sample)]} × 100.

Virus-specific antibody isotype ELISA. Sera were isolated and stored at −80°C. Total serum immunoglobulin Gs (IgGs) against TMEV were assessed by enzyme-linked immunosorbent assay (ELISA) as described previously (32). Purified virus was adsorbed to 96-well plates (Immulon II; Dynatech Laboratories Inc., Chantilly, VA) and then blocked with 1.0% bovine serum albumin (BSA; Sigma Chemical Co. St. Louis, MO) in phosphate-buffered saline. Serial serum dilutions were made in 0.2% BSA–phosphate-buffered saline and added in triplicate. Biotinylated anti-mouse IgG secondary antibodies were used for detection (Jackson Immunoresearch Labs, Westbury, NY). Signals were amplified with streptavidin-labeled alkaline-phosphatase (Jackson Immunoresearch Labs) and detected using *p*-nitrophenyl phosphate as the substrate. Absorbances were read at 405 nm and plotted against serum dilution factors. In addition, virus neutralization assays were performed to determine the serum concentration necessary to neutralize 90% of infectious virus by plaque assay on L2 cells.

Isolation of BILs. Brains from virus-infected mice were homogenized in 1 ml of RPMI 1640 and centrifuged in a 30% Percoll gradient at 10,000 rpm for 30 min at 4°C. Brain-infiltrating lymphocytes (BILs) at the bottom of the gradient were washed in RPMI by centrifugation at 1,500 rpm for 5 min at 4°C. BILs were resuspended in RPMI and depleted of red blood cells with a hypotonic solution and washed again to use in flow cytometry analysis.

TABLE 1. Spinal cord pathology of TMEV-infected mice at 18 days

Strain	No. of mice	% of quadrants with[a]:			No. of mice positive for demyelination/total (%)
		Gray matter disease	White matter inflammation	Demyelination	
$A\beta^0.\beta2m^0$	27	16.2 ± 1.9	5.7 ± 1.2	0.1 ± 0.1	1/27 (3.7)
$\beta2m^0$	10	1.5 ± 0.6	3.0 ± 0.7	3.7 ± 0.7	9/10 (90.0)
$A\beta^0$	13	0.0 ± 0.0	0.0 ± 0.0	0.0 ± 0.0	0/13 (0.0)
B6	15	0.0 ± 0.0	0.0 ± 0.0	0.3 ± 0.3	1/15 (6.6)
$A\beta^0.\beta2m^0$.DR2	12	4.8 ± 2.0	0.9 ± 0.6	0.0 ± 0.0	0/12 (0.0)
$A\beta^0.\beta2m^0$.DR3	7	0.4 ± 0.4	0.3 ± 0.3	0.0 ± 0.0	0/7 (0.0)
B10.Q	23	0.7 ± 0.3	10.1 ± 4.1	5.7 ± 2.2	13/23 (56.5)
SJL	6	0.0 ± 0.0	7.6 ± 2.3	7.3 ± 3.0	5/6 (83.3)

[a] Data are expressed as the percentage of spinal cord quadrants showing the pathological abnormality (mean ± standard error).

Flow cytometry analysis. BILs were incubated in 50 μl of fluorescence-activated cell sorter (FACS) medium (1% BSA and 0.02% sodium azide in Hanks' balanced salt solution) with anti-CD8a–fluorescein isothiocyanate (clone 53-6.7) and anti-CD4–phycoerythrin (clone H129.19) antibodies. BILs were washed three times in FACS medium and fixed in 2% paraformaldehyde. For evaluation of T-cell activation marker CD69, BILs were blocked for Fc receptor in 100 μl of medium from the $2.4G^2$ hybridoma. After blocking for 30 min, anti-CD45–allophycocyanin, CD4-phycoerythrin, and either CD69-fluorescein isothiocyanate or isotype control antibodies were added and incubated for 1 h on ice. BILs were washed two times in FACS medium and fixed in 2% paraformaldehyde. Flow cytometry was performed using a FACSCalibur flow cytometer (Becton Dickinson, San Diego, CA). Data were analyzed using WinMDI. Dead cells were excluded based on the forward scatter profile.

Statistics. Data were analyzed using either the Student's *t* test for normally distributed data or the Mann-Whitney rank sum test for data not normally distributed. Analysis of variance (ANOVA) was used for comparisons of more than one group. The Tukey or Dunn's test was used for all pairwise multiple comparison procedures. Proportional data were evaluated using the Z-test. The level for significance was set as $P < 0.05$ for all tests.

RESULTS

Transgenic expression of human class II HLA-DR prevents death in TMEV-infected $A\beta^0.\beta2m^0$ mice. Twenty-seven $A\beta^0.\beta2m^0$ mice were infected with TMEV, and all died or were moribund by 18 days postinfection. However, both β_2-microglobulin and class II-deficient mice had minimal neurologic deficits and survived past the 18-day time point, demonstrating that MHC class I and MHC class II can independently protect mice from early neurologic disease. Both $A\beta.\beta2m^0$.DR2 (n = 42) and $A\beta^0.\beta2m^0$.DR3 (n = 19) mice infected with TMEV survived past the 18-day time point without neurologic deficits. Thus, expression of human class II genes alone prevented the death of $A\beta^0.\beta2m^0$ mice following a lethal dose of TMEV.

Expression of human class II MHC transgenes prevents severe neuronal gray matter disease observed in the spinal cord of TMEV-infected $A\beta^0.\beta2m^0$ mice at 18 days postinfection. We calculated the percentage of spinal quadrants with neuronal injury in the gray matter disease, demyelination in the white matter, and inflammation in the white matter (Table 1; n = number of mice). We noted severe gray matter disease in the spinal cord of $A\beta^0.\beta2m^0$ mice. Gray matter disease was characterized by neuronal loss, intense inflammation around anterior horn cells, and vacuolar degeneration of neurons (Fig. 1). HLA transgenic mice infected with TMEV for 18 days revealed minimal gray matter spinal cord pathology in $A\beta^0.\beta2m^0$.DR2 (4.8 ± 2.0; n = 12) and $A\beta^0.\beta2m^0$.DR3 (0.4 ± 0.4; n = 7) mice. The decrease in gray matter disease in DR2

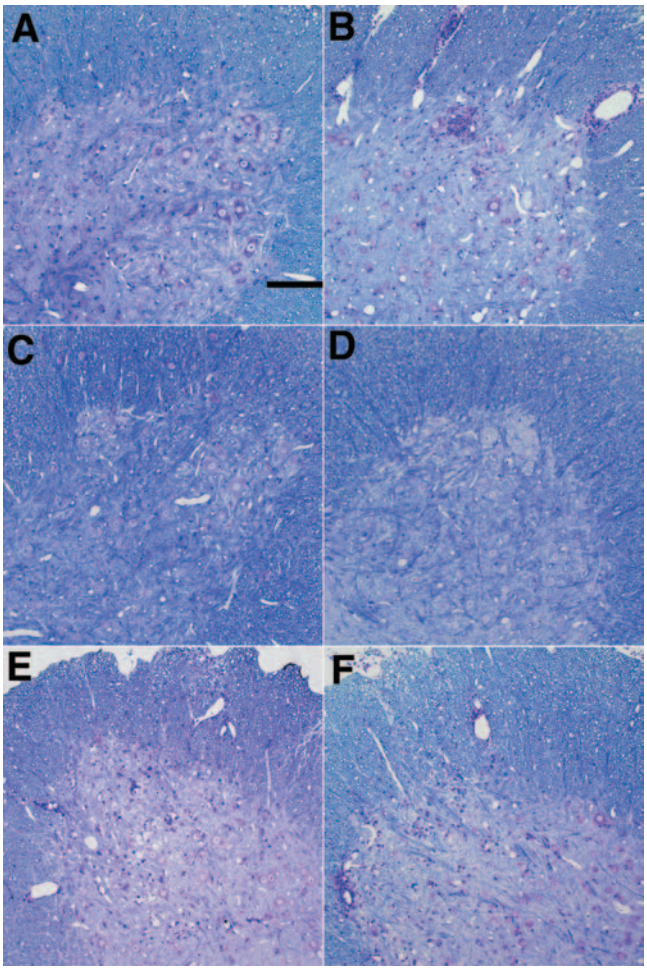

FIG. 1. Spinal cord pathology following TMEV infection (18 days). Glycol methacrylate plastic-embedded sections were stained with modified erichrome/cresyl violet stain. (A) Absence of gray matter pathology in B6 mouse. (B) Presence of inflammation and neuronal injury in the gray matter of an $A\beta^0.\beta2m^0$ mouse. (C) Absence of gray matter pathology in an $A\beta^0.\beta2m^0$.DR2 mouse. (D) Absence of gray matter pathology in an $A\beta^0.\beta2m^0$.DR3 mouse. (E) Presence of inflammation in the gray matter pathology in a $\beta2m^0$ mouse. (F) Presence of inflammation in the gray matter pathology in an $A\beta^0$ mouse.

TABLE 2. Spinal cord pathology of TMEV-infected mice at 45 days

Strain	No. of mice	% of quadrants with[a]:			No. of mice positive for demyelination/ total (%)	*P* value compared to $\beta2m^{0}$[b]
		Gray matter disease	White matter inflammation	Demyelination		
$\beta2m^{0}$	10	0.4 ± 0.3	8.1 ± 2.9	9.3 ± 2.4	10/10 (100)	
$A\beta^{0}$	19	0.5 ± 0.3	1.3 ± 0.7	4.9 ± 2.6	7/19 (36.8)	0.008
B10	11	0.0 ± 0.0	0.0 ± 0.0	0.0 ± 0.0	0/11 (0.0)	0.003
$A\beta^{0}.\beta2m^{0}$.DR2	7	0.0 ± 0.0	0.3 ± 0.3	1.2 ± 0.9	2/7 (28.6)	0.032
$A\beta^{0}.\beta2m^{0}$.DR3	5	0.0 ± 0.0	0.0 ± 0.0	0.4 ± 0.4	1/5 (20.0)	0.009
B10.Q	5	0.0 ± 0.0	11.1 ± 2.1	27.2 ± 6.3	6/6 (100)	0.007
SJL	18	0.3 ± 0.2	23.3 ± 3.5	23.3 ± 3.8	18/18 (100)	0.014

[a] Data are expressed as the percentage of spinal cord quadrants showing the pathological abnormality (mean ± standard error).
[b] Statistical significance determined for demyelination scores compared to those of $\beta2m^{0}$ mice by nonparametric rank sum test.

or DR3 transgenic mice compared to $A\beta^{0}.\beta2m^{0}$ mice was statistically significant (ANOVA on ranks, $P < 0.001$). Similarly low levels of gray matter disease were observed in $\beta2m^{0}$ mice and in $A\beta^{0}$ mice. Mild white matter inflammation was observed in $A\beta^{0}.\beta2m^{0}$ and $\beta2m^{0}$ mice, whereas essentially none was observed in DR2 or DR3 mice. Susceptible strains of B10.Q and SJL mice showed minimal gray matter disease, but, as expected, showed white matter inflammation and demyelination. Thus, expression of DR molecules was able to control the early gray matter disease observed in $A\beta^{0}.\beta2m^{0}$ mice.

Expression of DR transgene protects mice from spinal cord demyelination. We asked whether the expression of these human genes would influence chronic demyelination at 45 days following infection (Table 2 and Fig. 2). $A\beta^{0}.\beta2m^{0}$ mice were not available for these analyses, since none survived to this time point. $A\beta^{0}.\beta2m^{0}$.DR2 and $A\beta^{0}.\beta2m^{0}$.DR3 mice showed essentially no demyelination in the spinal cord following virus infection (Fig. 2 and Table 2). There was a significant decrease in quadrants showing demyelination in $A\beta^{0}.\beta2m^{0}$.DR2 or $A\beta^{0}.\beta2m^{0}$.DR3 mice compared to $\beta2m^{0}$ mice ($P < 0.001$). Our comparison with another DR allele, in $A\beta^{0}.\beta2m^{0}$.DR4 ($n = 4$) mice infected with TMEV, revealed no demyelination in any of 156 quadrants examined. In contrast, both $\beta2m^{0}$ mice (43) and $A\beta^{0}$ mice (32) showed low levels of demyelination in the spinal cord white matter. As expected, immunocompetent B6 mice ($n = 11$) showed no demyelination. Positive control B10.Q and SJL mice showed demyelination at this time point (Table 2).

Of the multiple littermate controls injected with TMEV to exclude for any other unknown genetic difference besides DR alleles, the following mice, as expected, did not show demyelination in the spinal cord at 45 days following Theiler's infection: $A\beta^{0}.\beta2m^{+/+}.DR2^{+}$ ($n = 3$), $A\beta^{0}.\beta2m^{+/-}.DR2^{+}$ ($n = 13$), $A\beta^{+}.\beta2m^{+/+}.DR3^{-}$ ($n = 7$), $A\beta^{+}.\beta2m^{0}.DR3^{+}$ ($n = 3$), $A\beta^{0}.\beta2m^{+/+}$. $DR3^{+}$ ($n = 12$), $A\beta^{0}.\beta2m^{+/+}.DR3^{+}$ ($n = 2$), and $A\beta^{0}.\beta2m^{+/+}.DR4^{+}$ ($n = 13$). In contrast and as expected, littermate controls with the $A\beta^{0}.\beta2m^{0}$ genotype died prior to the 18-day time point. These included the $A\beta^{0}.\beta2m^{0}.DR2^{0}$ ($n = 9$), $A\beta^{0}.\beta2m^{0}.DR3^{0}$ ($n = 3$), and $A\beta^{0}.\beta2m^{0}.DR4^{0}$ ($n = 4$) mice.

Expressions of DR2 or DR3 transgenes protect $A\beta^{0}.\beta2m^{0}$ mice from encephalitis following TMEV infection. We asked whether expression of DR2 or DR3 protected specific populations of brain cells from injury (Fig. 3). Analyzing the brain pathology at 18 days after infection (the time frame when $A\beta^{0}.\beta2m^{0}$ mice die) and using a semiquantitative four-point scale for analysis, we noted pathology in all strains (B6, $\beta2m^{0}$, $A\beta^{0}$, $A\beta^{0}.\beta2m^{0}$, $A\beta^{0}.\beta2m^{0}$.DR2, and $A\beta^{0}.\beta2m^{0}$.DR3) in the cortex, hippocampus, striatum, and corpus callosum, whereas there was no or minimal disease in the cerebellum (Fig. 3). Levels of meningeal inflammation were similar between the

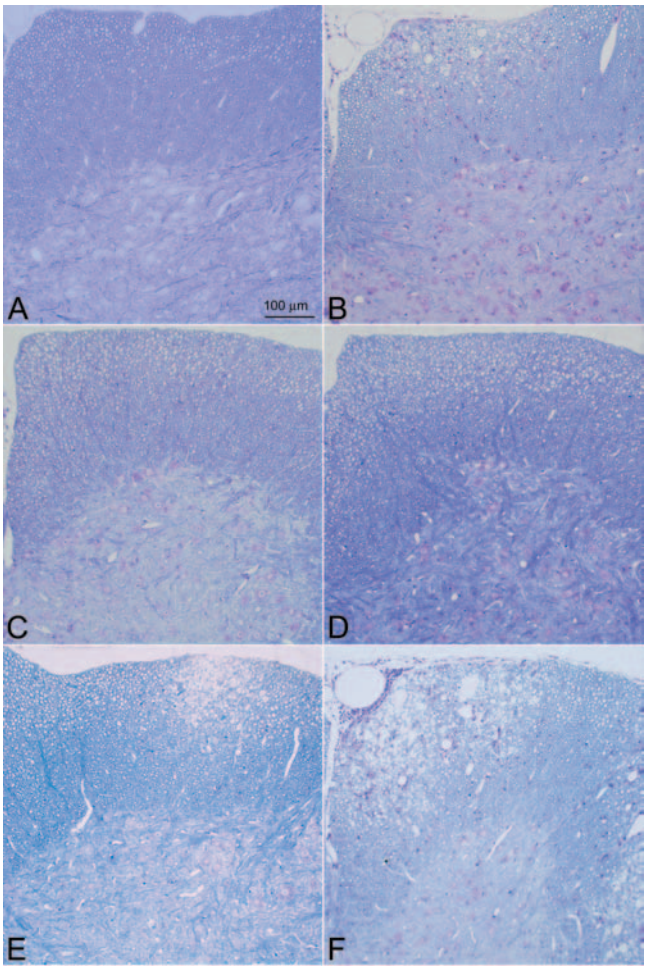

FIG. 2. Spinal cord pathology following TMEV infection (45 days). Glycol methacrylate plastic-embedded sections were stained with modified erichrome/cresyl violet stain. (A) Absence of white matter pathology in a B6 mouse. (B) Presence of inflammation and demyelination in a $\beta2m^{0}$ mouse. (C) Absence of white matter pathology in an $A\beta^{0}.\beta2m^{0}$.DR2 mouse. (D) Absence of white matter pathology in an $A\beta^{0}.\beta2m^{0}$.DR3 mouse. (E) Positive control showing demyelination in an SJL/J mouse. (F) Positive control showing demyelination in a B10.Q mouse.

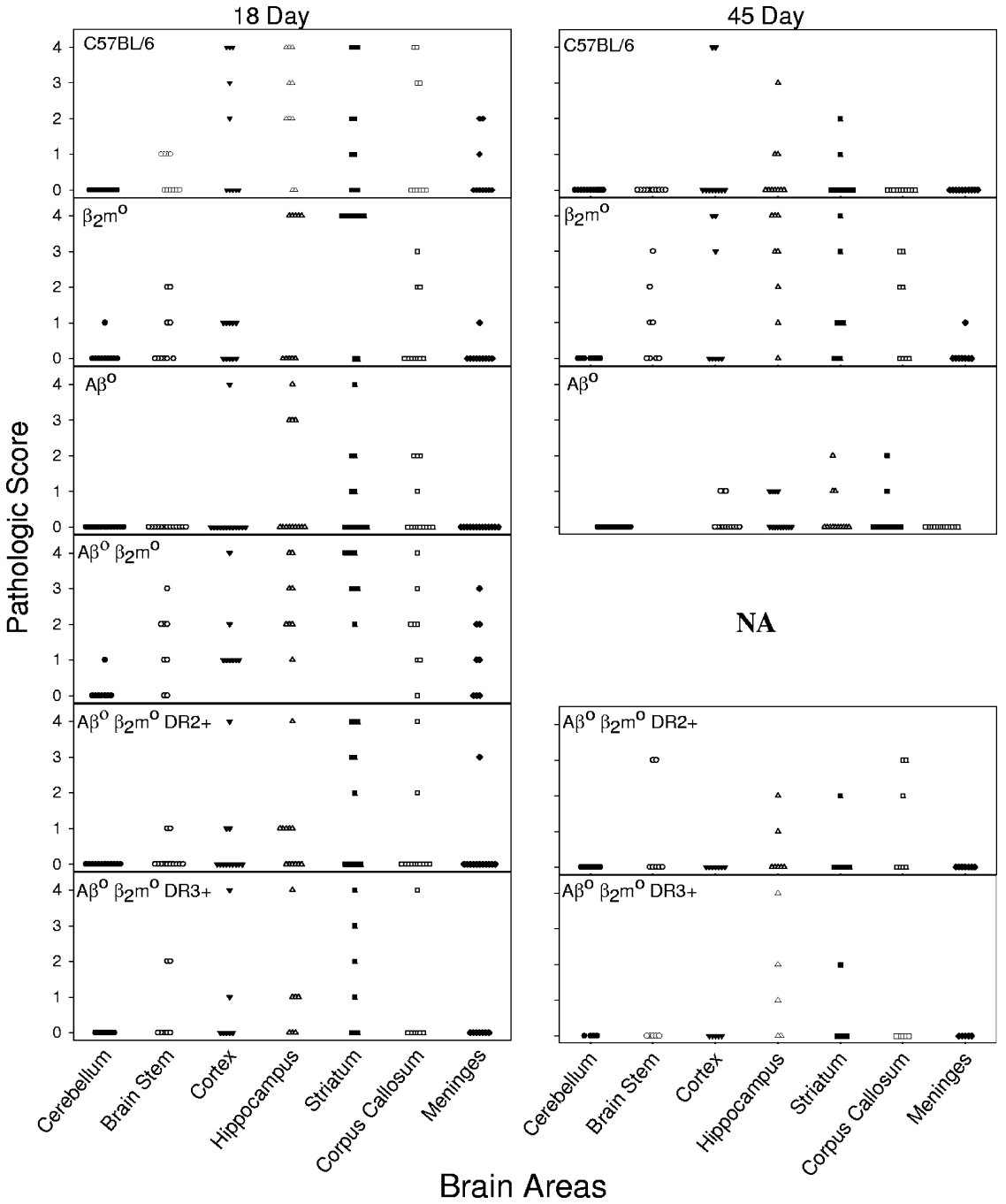

FIG. 3. Pathology of the brain. Pathological analysis of brain areas (cerebellum, brain stem, cortex, hippocampus, striatum, corpus callosum, and meninges) at 18 days and 45 days following TMEV infection. The mouse strains shown are B6, $\beta2m^0$, $A\beta^0$, $A\beta^0.\beta2m^0$, $A\beta^0.\beta2m^0$.DR2, and $A\beta^0.\beta2m^0$.DR3. Pathological qualitative scores from 0 to 4 are described in Materials and Methods. Each point represents one mouse. There were no differences between the strains in the distribution of brain pathologies at 18 days after infection. At the 45-day time point, data were not available (NA) for $A\beta^0.\beta2m^0$ mice because all of these mice were dead (or moribund and thus sacrificed for humane reasons) by 18 days after infection. These data are representative of two of the three experiments performed for each strain at each time point.

strains. There was less brain pathology at 18 days after infection in $A\beta^0.\beta2m^0$.DR2 mice (0.548 ± 0.128; $n = 84$) and in $A\beta^0.\beta2m^0$.DR3 mice (0.612 ± 0.175; $n = 49$) compared to $A\beta^0.\beta2\ m^0$ mice (1.750 ± 0.179; $n = 56$), which was statistically significant by ANOVA on ranks ($P < 0.001$). (n represents the number of brain areas examined.) There was a suggestion, which was not statistically significant, that $A\beta^0.\beta2m^0$ mice show more brain pathology in the brain stem.

We then analyzed the distribution of brain disease at 45 days after infection. $A\beta^0.\beta2m^0$.DR2 and $A\beta^0.\beta2m^0$.DR3 mice showed minimal brain pathology limited to the hippocampus and the striatum. By 45 days after infection, many animals

showed no brain pathology in the areas studied. None of 10 $A\beta^0.\beta2m^0$.DR2 and $A\beta^0.\beta2m^0$.DR3 mice showed meningeal inflammation. There was a gradual resolution of brain disease in $A\beta^0.\beta2m^0$.DR3 mice from 7 days (1.510 ± 0.157; $n = 84$), to 21 days (0.612 ± 0.175; $n = 49$), to 45 days (0.273 ± 0.146; $n = 33$), which was statistically significant by ANOVA on ranks ($P < 0.001$). At 45 days following infection, the brain pathological scores in $A\beta^0.\beta2m^0$.DR2 mice (0.337 ± 0.083; $n = 98$) and $A\beta^0.\beta2m^0$.DR3 mice (0.273 ± 0.146; $n = 33$) did not differ statistically from the scores for B6 mice that normally control virus infection (0.325 ± 0.086; $n = 126$).

As expected, B6 mice resolved brain disease when comparing the pathology at 7 days (2.000 ± 0.150; $n = 119$), 21 days (1.321 ± 0.141; $n = 140$), and 45 days (0.325 ± 0.086; $n = 126$). In contrast, in the $\beta2m^0$ strain, brain pathology persisted when comparing the results at 7 days (1.929 ± 0.249; $n = 56$), 21 days (1.029 ± 0.186; $n = 70$), and 45 days (1.071 ± 0.195; $n = 56$). There was a statistical difference in the increase in brain pathological scores comparing $\beta2m^0$ mice ($n = 56$) to B6 mice ($P < 0.001$, Mann-Whitney rank sum test). There was no statistical difference in the brain scores comparing B6 to $A\beta^0$ mice.

DR2 and DR3 transgenic mice have minimal virus antigen in the spinal cord during the late stages of disease. We concentrated our analysis on the gray matter of the spinal cord at 18 days after infection to evaluate the association of virus antigen with early death (Fig. 4). There were statistically more spinal cord quadrants with virus antigen in $A\beta^0.\beta2m^0$mice than in B6, $A\beta^0$, or $\beta2m^0$ mice. There were more spinal cord quadrants with virus in the gray matter at 18 days following infection in $A\beta^0.\beta2m^0$ mice than in $A\beta^0.\beta2m^0$.DR2 and $A\beta^0.\beta2m^0$.DR3 mice (ANOVA, $P = 0.008$). There were statistically fewer white matter quadrants with virus antigen in $A\beta^0.\beta2m^0$.DR2 and $A\beta^0.\beta2m^0$.DR3 mice than in $A\beta^0.\beta2m^0$ mice (ANOVA, $P < 0.05$).

We then analyzed the percentage of spinal cord quadrants with virus antigen in the white matter at the 45-day time point (Fig. 4). $A\beta^0.\beta2m^0$.DR3 mice (3.8 ± 2.0; $n = 5$) had minimal virus antigen in the white matter. There was a statistically significant decrease of virus antigen in the spinal white matter when comparing $A\beta^0.\beta2m^0$.DR3 to $\beta2m^0$ mice ($P = 0.032$). B6 mice, as expected, controlled virus infection and showed no antigen-positive cells in the spinal cord white matter. In contrast, both $A\beta^0$ and $\beta2m^0$ mice showed virus antigen in the white matter.

Levels of TMEV RNA in the brain and spinal cord at 7, 18, and 45 days following infection. Reports indicate that viral RNA persists following TMEV infection during chronic disease, even though it is difficult to detect infectious virus by plaque assay (53). We tested the hypothesis that control of virus RNA lessened CNS pathology in $A\beta^0.\beta2m^0$.DR3 mice (Fig. 5). We controlled all experiments for expression of GAPDH RNA, which was consistent among strains. The level of GAPDH RNA in the brain was $\log_{10}$ 7.40 ± 0.03 virus copies, and that in the spinal cords was $\log_{10}$ 7.01 ± 0.03 virus copies.

All strains of mice (B6, $\beta2m^0$, $A\beta^0$, $A\beta^0.\beta2m^0$, and $A\beta^0.\beta2m^0$.DR3) had high levels of virus RNA in the brain and spinal cord during the 7-day acute infection. There was no difference in the critical comparison of $A\beta^0.\beta2m^0$ with $A\beta^0.\beta2m^0$.DR3, indicating that these strains had equal capacity to replicate virus in the brain and spinal cord. Of interest, at the 18-day time point, $A\beta^0.\beta2m^0$.DR3 mice had less replication of virus in the brain (ANOVA on ranks, $P < 0.001$). There was no statistical difference between $A\beta^0.\beta2m^0$ and $A\beta^0.\beta2m^0$.DR3 in the virus RNA in the spinal cord. At the 45-day time point, $A\beta^0.\beta2m^0$.DR3 mice behaved more like resistant B6 mice than susceptible B10.Q mice (ANOVA on ranks, $P < 0.001$). Thus, the DR gene worked efficiently in the absence of $\beta2m^0$ to help control the viral load in the brain to prevent death in $A\beta^0.\beta2m^0$ mice. However, virus RNA persisted in the spinal cord of $A\beta^0.\beta2m^0$.DR3 mice, even though these mice showed minimal or no spinal cord demyelination.

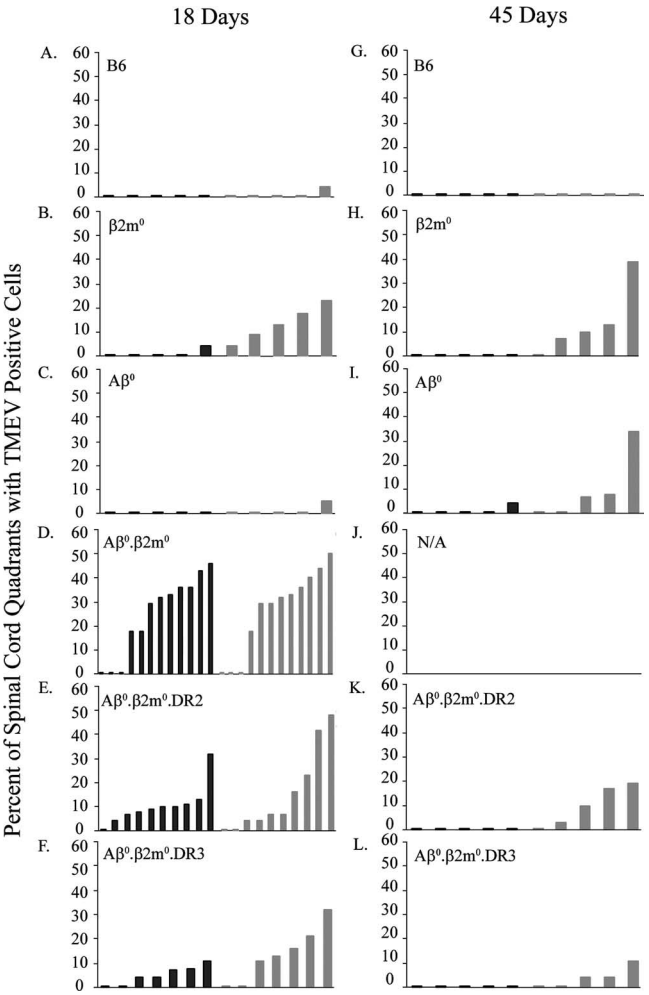

FIG. 4. Virus antigen-positive cells. Virus antigen-positive cells were determined by immunoperoxidase staining and expressed as the percentage of spinal quadrants showing virus antigen-positive cells in either the gray matter or the white matter. Twenty to thirty spinal cord quadrants were analyzed for each mouse. Analysis was done 18 days and 45 days after infection. Each bar represents one animal. (A) B6 mice (18 days). (B) $\beta2m^0$ mice (18 days). (C) $A\beta^0$ mice (18 days). (D) $A\beta^0.\beta2m^0$ mice (18 days). (E) $A\beta^0.\beta2m^0$.DR2 mice (18 days). (F) $A\beta^0.\beta2m^0$.DR3 mice (18 days). (G) B6 mice (45 days). (H) $\beta2m^0$ mice (45 days). (I) $A\beta^0$ mice (45 days). (J) $A\beta^0.\beta2m^0$.DR2 mice (45 days). (K) $A\beta^0.\beta2m^0$.DR3 mice (45 days). (L) N/A, no animals are available because all $A\beta^0.\beta2m^0$ mice died from TMEV infection by day 18.

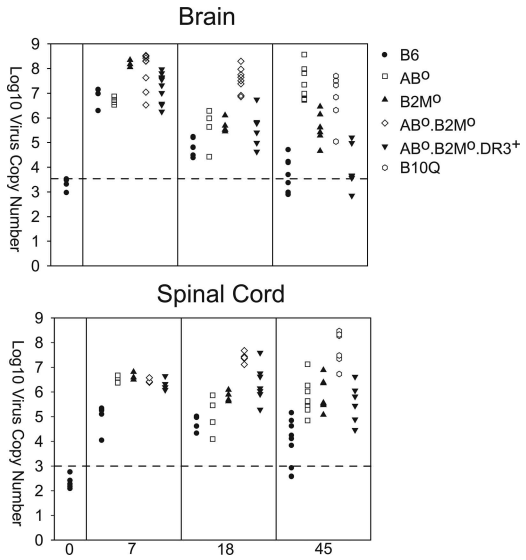

FIG. 5. Virus RNA expression. Levels of virus RNA expression in mice at 7, 18, and 45 days following TMEV infection analyzed independently in the brain and spinal cord. Levels of viral capsid RNA message were quantified by Light Cycler PCR using primers for capsid VP2. Each symbol represents the level from a single mouse. The levels of expression of GAPDH RNA were consistent among the groups (brains, $\log_{10}$ 7.40 ± 0.03 virus copies; spinal cords, $\log_{10}$ 7.01 ± 0.03 virus copies). The dotted line represents the sensitivity of the assay. Symbols along or below the line indicate animals with minimal or no detection of virus RNA.

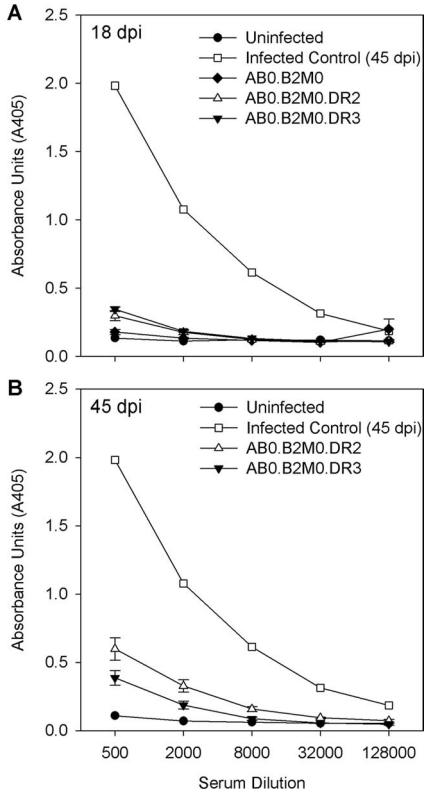

FIG. 6. Virus-specific humoral immune responses. Shown are the results of an ELISA for serum IgG antibodies at 18 and 45 days after infection directed against purified TMEV antigens in various strains of mice. Negative controls are from mice not infected with TMEV.

The humoral immune response to virus antigens does not explain the control of virus infection in DR transgenic mice. To test whether the difference in phenotype between Aβ^{0}.β2m^{0} mice (early virus replication and death) and Aβ^{0}.β2m^{0}.DR2 mice or Aβ^{0}.β2m^{0}.DR3 mice (virus control and minimal demyelination) resulted from differences in the humoral response to virus, we assessed serum IgG and IgM antibody responses by ELISA directed against purified virus antigens (Fig. 6) at 18 and 45 days after infection. Aβ^{0}.β2m^{0}.DR2 mice or Aβ^{0}.β2m^{0}.DR3 mice developed low-level IgM and IgG responses to purified virus, whereas Aβ^{0}.β2m^{0} mice did not mount a response. Noninfected littermate controls showed no antivirus antibody responses. Sera from Aβ^{0}.β2m^{0}.DR2 mice or Aβ^{0}.β2m^{0}.DR3 mice showed low serum-neutralizing antibody titers by neutralization plaque assay similar to sera from Aβ^{0}.β2m^{0} mice. The titer of sera required to neutralize 90% of viral plaques ranged from 1:64 to 1:128 in Aβ^{0}.β2m^{0}.DR2, Aβ^{0}.β2m^{0}.DR3, or Aβ^{0}.β2m^{0} mice. In contrast, in infected B10.Q or B6 mice, the titers were >1:2,048. Thus, strong neutralizing antibody responses to the virus do not explain why Aβ^{0}.β2m^{0}.DR2 mice or Aβ^{0}.β2m^{0}.DR3 mice control virus infection and survive the acute encephalitis.

DR transgenic mice show CD4^{+} T cells in the CNS following TMEV infection. No CD4^{+} or CD8^{+} T cells were observed in the brain infiltrates of Aβ^{0}.β2m^{0} mice (data not shown). In contrast, CD4^{+} T cells were observed in the infiltrate of all Aβ^{0}.β2m^{0}.DR3 or β2m^{0} mice (Fig. 7). There were fewer CD4^{+} T cells in the brain infiltrates of Aβ^{0}.β2m^{0}.DR3 mice than in β2m^{0} mice (Fig. 7). None of the Aβ^{0}.β2m^{0}.DR3 or β2m^{0} mice had CD8^{+} T cells in the brain infiltrate. The data indicate that the control of virus infection in Aβ^{0}.β2m^{0}.DR3 mice probably depends on CD4^{+} T cells. These cells may have acted alone or, more likely, in concert with other cells (macrophages, microglia, and astrocytes) to control virus infection and prevent chronic demyelination.

Cytokine expression in the brain of DR transgenic mice may explain the mechanism of control in virus infection. Cytokine analysis from 7-day-infected mice (Fig. 8) showed both B6 and Aβ^{0}.β2m^{0}.DR3 mice to have significantly higher IFN-γ levels than Aβ^{0}.β2m^{0} mice ($P < 0.001$). The DR3 transgenic mice also showed a significant increase in IL-2 transcripts compared to Aβ^{0}.β2m^{0}mice ($P < 0.05$), which was similar to that observed in B6 mice. IL-4 was increased in B6 mice compared to Aβ^{0}.β2m^{0} mice ($P < 0.05$). However, levels of IL-4 transcripts in DR3 transgenic mice were closer to values in Aβ^{0}.β2m^{0} mice. By day 18, expression levels of IFN-γ and IL-2 in both B6 and DR3 mice were reduced to the levels seen in the Aβ^{0}.β2m^{0} mice (Fig. 8), which correlate with the reduced levels of virus RNA seen in the brains of both strains at this time. At 18 days, there was an increase in IL-6 ($P < 0.001$) and TNF-α ($P < 0.05$) in the brains of Aβ^{0}.β2m^{0} mice compared to B6 and DR3 transgenic mice. The data support the hypothesis that activated CD4 cells infiltrating the brain of Aβ^{0}.β2m^{0}.DR3 mice at 7 days expressed the cytokines IFN-γ and IL-2 to control virus infection. The increased expression of IL-6 and TNF-α in brains of Aβ^{0}.β2m^{0} mice supports the possibility that these cytokines contribute to the severe pathology and death ob-

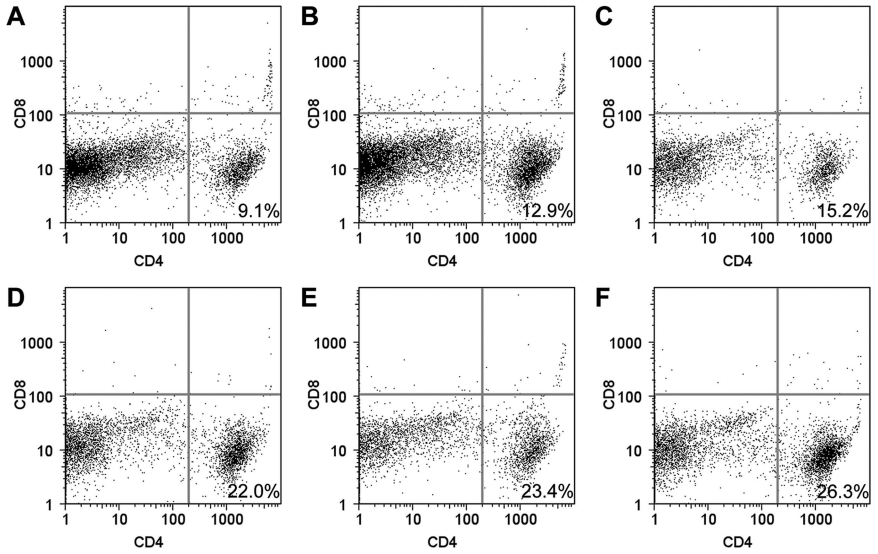

FIG. 7. FACS analyses of BILs. Mice were infected for 7 days with TMEV, and then BILs were isolated using a Percoll gradient. Cells were double labeled for CD4 or CD8 and analyzed by cell sorting. The number shown in the lower left quadrant of each panel represents the percentage of BILs positive for the CD4 marker. Note that no $CD8^+$ T cells were present in the BILs from either $A\beta^0.\beta2m^0$.DR3 (A, B, and C) or $\beta2m^0$ (D, E, and F) mice.

served in the virus-infected $A\beta^0.\beta2m^0$ mice. Finally, we demonstrate that the $CD4^+$ T cells infiltrating the brain are activated, since they are expressed on the surface CD69 antigen.

DISCUSSION

This study indicates that a human class II gene, in this case either DR2 or DR3, can control virus infection in a host without the contribution of the class I immune response. Transgenic expression of either DR2 or DR3 in $A\beta^0.\beta2m^0$ mice prevents the phenotypic consequence of persistent viral antigen expression—in this case, chronic spinal cord demyelination. Of significance, the level of protection toward chronic spinal cord demyelination observed in $A\beta^0.\beta2m^0$.DR2 or $A\beta^0.\beta2m^0$.DR3 mice is greater than that observed in $\beta2m^0$ mice with endogenous mouse class II *H-2*^{b} alleles. This is unexpected and suggests that the human DR2 or DR3 gene, in this scenario, may function more efficiently than the endogenous mouse class II *H-2*^{b} alleles. This occurs despite the fact that these mice have otherwise an immune repertoire of mouse T cells and mouse T cell receptors. This is consistent with the hypothesis that human DR molecules, via the secretion of cytokines, are critical in controlling virus replication in the host. The data demonstrate increased transcription of IL-2 and IFN-γ in the brain of DR transgenic mice following infection.

Infection with Theiler's virus in most mouse strains studied to date usually results in two distinct phenotypes. In animals that do not develop demyelination, such as prototypic C57BL/6 mice, virus replicates in the brain during the first 7 to 10 days of infection, resulting in encephalitis involving the hippocampus, striatum, and cortex. The virus then clears rapidly from the brain following an intense inflammatory response (19) that precludes virus antigen expression and subsequent demyelination in the spinal cord. This protective response has been mapped genetically to *H-2D* genes by recombinant inbred strains (44) or with transgenic mice (42). In resistant mice, the $CD8^+$ T-cell response is directed against an immunodominant viral peptide on VP2 that participates in virus clearance (1, 4, 12, 18, 26) Other investigators have studied Theiler's infection in BALB/c mice and have shown that $CD8^+$ T cells play a protective role, possibly as suppressor cells (10, 29). In animals that develop demyelination, such as the prototypic SJL/J or B10.Q mice, similar early encephalitis occurs in the brain. However, in these mice, the virus antigen persists in glial cells and macrophages of the spinal cord after it clears from the brain. In susceptible mice, activated cytotoxic T cells are generated in the brain (20) without apparent viral or myelin specificity (17). Demyelination in association with an intense inflammatory response, which begins in the spinal cord around day 21 following infection, is well established by day 45. Demyelination continues to worsen until 100 days after infection but then reaches a plateau (24). However, the animals continue to worsen neurologically for another subsequent 100 days after infection as a result of loss of large-diameter axons from the spinal cord (24).

This set of experiments with DR2 and DR3 transgenic mice challenges the model proposed by our lab and others that class I-restricted cytotoxic T lymphocytes are absolutely required for viral control of TMEV infection. Replacement of the endogenous class II allele with either DR2 or DR3 in $A\beta^0.\beta2m^0$ results not only in survival of mice from acute encephalitis but also prevention of virus antigen persistence in the spinal cord white matter. Despite the absence of virus antigen persistence in the spinal cord, these DR transgenic mice did show virus persistence in the spinal cord as documented by quantitative RT-PCR. The $A\beta^0.\beta2m^0$.DR2 or $A\beta^0.\beta2m^0$.DR3 mice did not develop chronic demyelination. Therefore, these mice did not behave like their expected counterparts, $\beta2m^0$ mice. Instead, these mice behaved pathologically like B6 mice, which control infection. FACS analyses of the cells infiltrating the CNS from

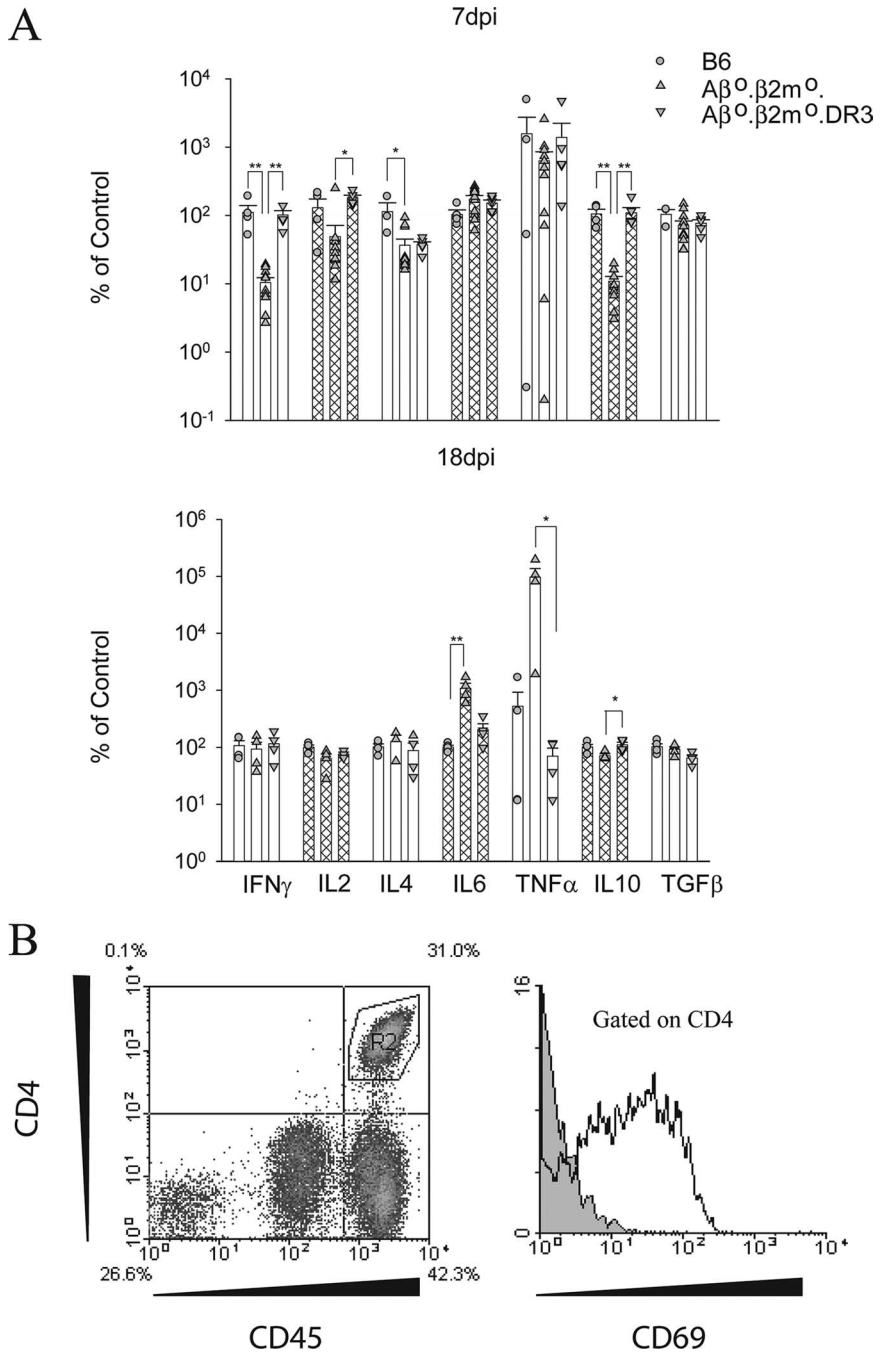

FIG. 8. BILs from $A\beta^0.\beta2m^0$.DR3 mice contain activated $CD4^+$ T cells and express similar inflammatory cytokines to B6 mice. (A) RNA transcripts of cytokines in brains of mice at 7 and 18 days postinfection were measured by quantitative real-time RT-PCR. Data are shown as a percentage of transcripts relative to the B6 mice for each gene, and all data are normalized to GAPDH. Each bar represents data from five animals. *, $P < 0.05$; **, $P < 0.001$. (B) Flow cytometry of BILs from an $A\beta^0.\beta2M^0$.DR3 mouse. $CD4^+$ T cells from the left panel are gated, and CD69 expression levels are shown on the right panel. The gray histogram represents the isotype control antibody.

DR transgenic mice showed $CD4^+$ T cells but not $CD8^+$ T cells. The $CD4^+$ cells in the brain were activated to an unknown antigen, since they expressed CD69 on their surface (56–58). Thus, the DR2 or DR3 molecule by itself was able to protect from chronic demyelination. This is supported by previous data that indicate a critical role of CD4 T cells in clearance (13, 16, 47). However, in the previous situations, it was not possible to determine if CD4 T cells alone contributed to this response, since these mice had functional CD8 T-cell compartments.

Previous studies have demonstrated that class I-deficient mice ($\beta2m^0$) (7, 39) or class II-deficient mice ($A\beta^0$) (8, 32) survive and clear the brain of encephalitis but, with time, develop spinal cord demyelination. The present study confirms

these results. The results from the $\beta 2m^0$ or $A\beta^0$ mice indicate that neither $CD4^+$ T cells nor $CD8^+$ T cells are required independently for early limitation of virus replication in the brain, since these mice survive the acute infection. However, both strains of mice fail to control the infection, and virus antigen persists in the spinal cord white matter. In addition, the results from $\beta 2m^0$ or $A\beta^0$ mice indicate that neither class II-restricted cells nor class I-restricted T cells independently are required for subsequent demyelination. This has been confirmed by CD4 and CD8 knockout mice (28) and contrasts with infection of doubly deficient $A\beta^0.\beta 2m^0$ mice; the latter fail to control the acute virus encephalitis and die before demyelination can ensue in the spinal cord (34).

The present experiments contrast with previous experiments performed in our laboratory using $A\beta^0.\beta 2m^0$.DQ6 or $A\beta^0.\beta 2m^0$.DQ8 mice. Following TMEV infection, DQ6 and DQ8 mice did not control virus infection and developed late-onset demyelination in the spinal cord. It is unclear why they demyelinate, whereas $A\beta^0.\beta 2m^0$.DR2 or $A\beta^0.\beta 2m^0$.DR3 mice do not. Clearly, DQ molecules do not provide the same level of protection as DR in mice following infection. This may have implications in human diseases where there is preferential influence on incidence or severity of symptoms dependent on the human class II alleles.

We do not know the precise mechanisms by which the DR2 or DR3 molecule by itself provides complete protection from chronic virus disease. Our laboratory is exploring several possibilities and has made significant progress in excluding the following. (i) Expression of human DR2 or DR3 may have resulted in the generation of class II-restricted cytotoxic lymphocytes against the virus. Class II-restricted cytotoxic lymphocytes restricted to human DR or DQ have been described in some other model systems (6, 22, 30, 59). However their presence is rare. We show in this paper that CD4 cells are activated, since they express the CD69 antigen. (ii) Expression of DR molecules may have generated $CD4^+$ T cells that recognize viral peptides and secreted protective molecules to limit virus infection and prevent neuronal injury. The Theiler's model system provides possible evidence that IFN-γ (27, 40, 46), IL-6 (35), and TNF (36) are immune response-induced factors critical in controlling virus infection. We show in this paper that the DR transgenic mice secrete IFN-γ and IL-2 early in infection, which may contribute to virus replication control. (iii) DR-restricted $CD4^+$ T cells may help B cells to secrete protective and neutralizing antibody to help control the virus infection. However, TMEV-infected $A\beta^0.\beta 2m^0$.DR2 or $A\beta^0.\beta 2m^0$.DR3 mice do not develop strong antibody-neutralizing titers to TMEV. (iv) DR molecules on macrophages or dendritic cells may function independently of T cells to promote virus control. This seems unlikely because CD4 T cells were activated in the lesion and were the predominant cell type in the infiltrate.

There are some precedents for human DR molecules influencing the course of Theiler's infection in animals. Transgenic expression of DR3 molecules in mice of a susceptible B10.M ($H\text{-}2^f$) haplotype developed less demyelination than littermate controls without the DR3 transgene (5). These experiments differed from the present experiments in that the parental mice were immune competent and of a haplotype that develops demyelination. In the B10M.DR3 experiments, we could not exclude the DR3 transgene from interacting with the mouse immune system (for example, generation of a more robust mouse class I immune response) to account for the reduction of demyelination. Nevertheless, the protective qualities of DR3 discovered in previous experiments support the current findings.

There are precedents for human DR molecules influencing the course of virus, parasite, or spirochete infection in humans. Human cytomegalovirus protein pp65 has been shown to down-regulate HLA-DR induction by causing DR accumulations in lysosomes with subsequent destruction of the HLA-DR alpha chain (33). MHC class II allele (DRB1*1302) is associated with clearance of hepatitis B virus in The Gambia. In the infection with hepatitis C, DRB*0101-DQB1*0501 is associated with viral clearance, whereas DRB1*03011-DQB1*0201 is associated with chronic infection. Racial differences in the HLA class II association with hepatitis C virus may contribute to outcomes (52). DRB1*01 and DRB1*017(03) have been associated with acute disseminated encephalomyelitis in children, a disease in which an autoimmune reaction occurs in the CNS as a result of a viral trigger (11). In visceral leishmaniasis, HLA-DR2 is protective (25). In contrast, prominent MHC class II associations have not been observed in another parasitic infection, malaria (54). In spirochete infection resulting in Lyme's disease, HLA-DR7 allele is associated with highest antibody production against *Borrelia burgdorferi* (55).

Even though strong epidemiological data associate human MHC haplotype with the outcome to infectious disease, it has not been possible to prove conclusively that a human class II gene alone influences the consequences of infection. This is because human HLA is a complex haplotype, and there is linkage disequilibrium between alleles. Because our studies used transgenic mice with a single human class II transgene without either the mouse endogenous class I or class II response, we are in a stronger position to conclude that molecules within the class II MHC complex directly influence the course of a viral infection in vivo.

ACKNOWLEDGMENTS

This work was supported by National Institutes of Health grants P01 NS 38468 and R01 NS 32129 and National MS Society Center grants CA 1011A8 and RG3172.

Lea Dacy helped edit the manuscript.

REFERENCES

1. **Borson, N. D., C. Paul, X. Lin, W. K. Nevala, M. A. Strausbauch, M. Rodriguez, and P. J. Wettstein.** 1997. Brain-infiltrating cytolytic T lymphocytes specific for Theiler's virus recognize $H2D^b$ molecules complexed with a viral VP2 peptide lacking a consensus anchor residue. J. Virol. **71:**5244–5250.
2. **Dal Canto, M. C., and H. L. Lipton.** 1982. Ultrastructural immunohistochemical localization of virus in acute and chronic demyelinating Theiler's virus infection. Am. J. Pathol. **106:**20–29.
3. **Dal Canto, M. C., and S. G. Rabinowitz.** 1982. Experimental models of virus-induced demyelination of the central nervous system. Ann. Neurol. **11:**109–127.
4. **Dethlefs, S., N. Escriou, M. Brahic, S. van der Werf, and E. L. Larsson-Sciard.** 1997. Theiler's virus and Mengo virus induce cross-reactive cytotoxic T lymphocytes restricted to the same immunodominant VP2 epitope in C57BL/6 mice. J. Virol. **71:**5361–5365.
5. **Drescher, K. M., L. T. Nguyen, V. Taneja, M. J. Coenen, J. L. Leibowitz, G. Strauss, G. J. Hammerling, C. S. David, and M. Rodriguez.** 1998. Expression of the human histocompatibility leukocyte antigen DR3 transgene reduces the severity of demyelination in a murine model of multiple sclerosis. J. Clin. Investig. **101:**1765–1774.

6. **Faber, L. M., S. A. van Luxemburg-Heijs, W. F. Veenhof, R. Willemze, and J. H. Falkenburg.** 1995. Generation of CD4+ cytotoxic T-lymphocyte clones from a patient with severe graft-versus-host disease after allogeneic bone marrow transplantation: implications for graft-versus-leukemia reactivity. Blood **86:**2821–2828.
7. **Fiette, L., C. Aubert, M. Brahic, and C. Peña Rossi.** 1993. Theiler's virus infection of β_2-microglobulin-deficient mice. J. Virol. **67:**589–592.
8. **Fiette, L., M. Brahic, and C. Pena-Rossi.** 1996. Infection of class II-deficient mice by the DA strain of Theiler's virus. J. Virol. **70:**4811–4815.
9. **Griffin, D. E., S. Ubol, P. Despres, T. Kimura, and A. Byrnes.** 2001. Role of antibodies in controlling alphavirus infection of neurons. Curr. Top. Microbiol. Immunol. **260:**191–200.
10. **Haynes, L. M., C. L. Vanderlugt, M. C. Dal Canto, R. W. Melvold, and S. D. Miller.** 2000. $CD8^+$ T cells from Theiler's virus-resistant BALB/CBYJ mice downregulate pathogenic virus-specific $CD4^+$ T cells. J. Neuroimmunol. **106:**43–52.
11. **Idrissova, Z. R., M. N. Boldyreva, E. P. Dekonenko, N. A. Malishev, I. Y. Leontyeva, I. N. Martinenko, and A. S. Petrukhin.** 2003. Acute disseminated encephalomyelitis in children: clinical features and HLA-DR linkage. Eur. J. Neurol. **10:**537–546.
12. **Johnson, A. J., M. K. Njenga, M. J. Hansen, S. T. Kuhns, L. Chen, M. Rodriguez, and L. R. Pease.** 1999. Prevalent class I-restricted T-cell response to the Theiler's virus epitope D^b:$VP2_{121–130}$ in the absence of endogenous CD4 help, tumor necrosis factor alpha, gamma interferon, perforin, or costimulation through CD28. J. Virol. **73:**3702–3708.
13. **Karls, K. A., P. W. Denton, and R. W. Melvold.** 2002. Susceptibility to Theiler's murine encephalomyelitis virus-induced demyelinating disease in BALB/CANNCR mice is related to absence of a CD4+ T-cell subset. Mult. Scler. **8:**469–474.
14. **Khare, M., M. Rodriguez, and C. S. David.** 2003. HLA class II transgenic mice authenticate restriction of myelin oligodendrocyte glycoprotein-specific immune response implicated in multiple sclerosis pathogenesis. Int. Immunol. **15:**535–546.
15. **Levy, M., C. Aubert, and M. Brahic.** 1992. Theiler's virus replication in brain macrophages cultured in vitro. J. Virol. **66:**3188–3193.
16. **Lin, X., X. Ma, M. Rodriguez, and R. P. Roos.** 2004. CD4+ T cells are important for clearance of DA strain of TMEV from the central nervous system of SJL/J. mice. Int. Immunol. **16:**1237–1240.
17. **Lin, X., L. R. Pease, P. D. Murray, and M. Rodriguez.** 1998. Theiler's virus infection of genetically susceptible mice induces central nervous system-infiltrating CTLs with no apparent viral or major myelin antigenic specificity. J. Immunol. **160:**5661–5668.
18. **Lin, X., N. R. Thiemann, L. R. Pease, and M. Rodriguez.** 1995. VP1 and VP2 capsid proteins of Theiler's virus are targets of H-2D-restricted cytotoxic lymphocytes in the central nervous system of B10 mice. Virology **214:**91–99.
19. **Lindsley, M. D., and M. Rodriguez.** 1989. Characterization of the inflammatory response in the central nervous system of mice susceptible or resistant to demyelination by Theiler's virus. J. Immunol. **142:**2677–2682.
20. **Lindsley, M. D., R. Thiemann, and M. Rodriguez.** 1991. Cytotoxic T cells isolated from the central nervous systems of mice infected with Theiler's virus. J. Virol. **65:**6612–6620.
21. **Lipton, H. L.** 1975. Theiler's virus infection in mice: an unusual biphasic disease process leading to demyelination. Infect. Immun. **11:**1147–1155.
22. **Littaua, R. A., M. B. Oldstone, A. Takeda, and F. A. Ennis.** 1992. A $CD4^+$ cytotoxic T-lymphocyte clone to a conserved epitope on human immunodeficiency virus type 1 p24: cytotoxic activity and secretion of interleukin-2 and interleukin-6. J. Virol. **66:**608–611.
23. **Mangalam, A. K., M. Khare, C. Krco, M. Rodriguez, and C. David.** 2004. Identification of T cell epitopes on human proteolipid protein and induction of experimental autoimmune encephalomyelitis in HLA class II-transgenic mice. Eur. J. Immunol. **34:**280–290.
24. **McGavern, D. B., P. D. Murray, C. Rivera-Quinones, J. D. Schmelzer, P. A. Low, and M. Rodriguez.** 2000. Axonal loss results in spinal cord atrophy, electrophysiological abnormalities and neurological deficits following demyelination in a chronic inflammatory model of multiple sclerosis. Brain **123:** 519–531.
25. **Meddeb-Garnaoui, A., S. Gritli, S. Garbouj, M. Ben Fadhel, R. El Kares, L. Mansour, B. Kaabi, L. Chouchane, A. Ben Salah, and K. Dellagi.** 2001. Association analysis of HLA-class II and class III gene polymorphisms in the susceptibility to Mediterranean visceral leishmaniasis. Hum. Immunol. **62:** 509–517.
26. **Mendez-Fernandez, Y. V., A. J. Johnson, M. Rodriguez, and L. R. Pease.** 2003. Clearance of Theiler's virus infection depends on the ability to generate a CD8+ T cell response against a single immunodominant viral peptide. Eur. J. Immunol. **33:**2501–2510.
27. **Murray, P. D., D. B. McGavern, L. R. Pease, and M. Rodriguez.** 2002. Cellular sources and targets of IFN-gamma-mediated protection against viral demyelination and neurological deficits. Eur. J. Immunol. **32:**606–615.
28. **Murray, P. D., K. D. Pavelko, J. Leibowitz, X. Lin, and M. Rodriguez.** 1998. $CD4^+$ and $CD8^+$ T cells make discrete contributions to demyelination and neurologic disease in a viral model of multiple sclerosis. J. Virol. **72:**7320–7329.
29. **Nicholson, S. M., L. M. Haynes, C. L. Vanderlugt, S. D. Miller, and R. W. Melvold.** 1999. The role of protective CD8+ T cells in resistance of BALB/C mice to Theiler's murine encephalomyelitis virus-induced demyelinating disease: regulatory vs. lytic. J. Neuroimmunol. **98:**136–146.
30. **Nishimura, M., S. Mitsunaga, T. Akaza, Y. Mitomi, K. Tadokoro, and T. Juji.** 1994. Alloreactive feature of HLA-DP-specific cytotoxic T-cell clone. Cell. Immunol. **153:**262–270.
31. **Njenga, M. K., K. Asakura, S. F. Hunter, P. Wettstein, L. R. Pease, and M. Rodriguez.** 1997. The immune system preferentially clears Theiler's virus from the gray matter of the central nervous system. J. Virol. **71:**8592–8601.
32. **Njenga, M. K., K. D. Pavelko, J. Baisch, X. Lin, C. David, J. Leibowitz, and M. Rodriguez.** 1996. Theiler's virus persistence and demyelination in major histocompatibility complex class II-deficient mice. J. Virol. **70:**1729–1737.
33. **Odeberg, J., B. Plachter, L. Branden, and C. Soderberg-Naucler.** 2003. Human cytomegalovirus protein pp65 mediates accumulation of HLA-DR in lysosomes and destruction of the HLA-DR alpha-chain. Blood **101:**4870–4877.
34. **Pavelko, K. D., K. M. Drescher, D. B. McGavern, C. S. David, and M. Rodriguez.** 2000. HLA-DQ polymorphism influences progression of demyelination and neurologic deficits in a viral model of multiple sclerosis. Mol. Cell Neurosci. **15:**495–509.
35. **Pavelko, K. D., C. L. Howe, K. M. Drescher, J. D. Gamez, A. J. Johnson, T. Wei, R. M. Ransohoff, and M. Rodriguez.** 2003. Interleukin-6 protects anterior horn neurons from lethal virus-induced injury. J. Neurosci. **23:**481–492.
36. **Paya, C. V., P. J. Leibson, A. K. Patick, and M. Rodriguez.** 1990. Inhibition of Theiler's virus-induced demyelination in vivo by tumor necrosis factor alpha. Int. Immunol. **2:**909–913.
37. **Paya, C. V., A. K. Patick, P. J. Leibson, and M. Rodriguez.** 1989. Role of natural killer cells as immune effectors in encephalitis and demyelination induced by Theiler's virus. J. Immunol. **143:**95–102.
38. **Pierce, M. L., and M. Rodriguez.** 1989. Erichrome stain for myelin on osmicated tissue embedded in glycol methacrylate plastic. J. Histotechnol. **12:**35–36.
39. **Pullen, L. C., S. D. Miller, M. C. Dal Canto, and B. S. Kim.** 1993. Class I-deficient resistant mice intracerebrally inoculated with Theiler's virus show an increased T cell response to viral antigens and susceptibility to demyelination. Eur. J. Immunol. **23:**2287–2293.
40. **Pullen, L. C., S. D. Miller, M. C. Dal Canto, P. H. Van der Meide, and B. S. Kim.** 1994. Alteration in the level of interferon-gamma results in acceleration of Theiler's virus-induced demyelinating disease. J. Neuroimmunol. **55:**143–152.
41. **Rodriguez, M., and C. S. David.** 1985. Demyelination induced by Theiler's virus: influence of the H-2 haplotype. J. Immunol. **135:**2145–2148.
42. **Rodriguez, M., and C. S. David.** 1995. H-2 DD transgene suppresses Theiler's virus-induced demyelination in susceptible strains of mice. J. Neurovirol. **1:**111–117.
43. **Rodriguez, M., A. J. Dunkel, R. L. Thiemann, J. Leibowitz, M. Zijlstra, and R. Jaenisch.** 1993. Abrogation of resistance to Theiler's virus-induced demyelination in H-2b mice deficient in beta 2-microglobulin. J. Immunol. **151:**266–276.
44. **Rodriguez, M., J. Leibowitz, and C. S. David.** 1986. Susceptibility to Theiler's virus-induced demyelination. Mapping of the gene within the H-2D region. J. Exp. Med. **163:**620–631.
45. **Rodriguez, M., J. L. Leibowitz, and P. W. Lampert.** 1983. Persistent infection of oligodendrocytes in Theiler's virus-induced encephalomyelitis. Ann. Neurol. **13:**426–433.
46. **Rodriguez, M., K. Pavelko, and R. L. Coffman.** 1995. Gamma interferon is critical for resistance to Theiler's virus-induced demyelination. J. Virol. **69:** 7286–7290.
47. **Rodriguez, M., R. P. Roos, D. McGavern, L. Zoecklein, K. Pavelko, H. Sang, and X. Lin.** 2000. The CD4-mediated immune response is critical in determining the outcome of infection using Theiler's viruses with VP1 capsid protein point mutations. Virology **275:**9–19.
48. **Rodriguez, M., L. J. Zoecklein, C. L. Howe, K. D. Pavelko, J. D. Gamez, S. Nakane, and L. M. Papke.** 2003. Gamma interferon is critical for neuronal viral clearance and protection in a susceptible mouse strain following early intracranial Theiler's murine encephalomyelitis virus infection. J. Virol. **77:** 12252–12265.
49. **Rossi, C. P., M. Delcroix, I. Huitinga, A. McAllister, N. van Rooijen, E. Claassen, and M. Brahic.** 1997. Role of macrophages during Theiler's virus infection. J. Virol. **71:**3336–3340.
50. **Selin, L. K., S. M. Varga, I. C. Wong, and R. M. Welsh.** 1998. Protective heterologous antiviral immunity and enhanced immunopathogenesis mediated by memory T cell populations. J. Exp. Med. **188:**1705–1715.
51. **Sidman, R. L., J. B. Angevine, and E. T. Pierce.** 1971. Atlas of the mouse brain and spinal cord. Harvard University Press, Cambridge, MA.
52. **Thio, C. L., D. L. Thomas, J. J. Goedert, D. Vlahov, K. E. Nelson, M. W. Hilgartner, S. J. O'Brien, P. Karacki, D. Marti, J. Astemborski, and M. Carrington.** 2001. Racial differences in HLA class II associations with hepatitis C virus outcomes. J. Infect. Dis. **184:**16–21.

53. **Trottier, M., P. Kallio, W. Wang, and H. L. Lipton.** 2001. High numbers of viral RNA copies in the central nervous system of mice during persistent infection with Theiler's virus. J. Virol. **75:**7420–7428.
54. **Troye-Blomberg, M., O. Olerup, A. Larsson, K. Sjoberg, H. Perlmann, E. Riley, J. P. Lepers, and P. Perlmann.** 1991. Failure to detect MHC class II associations of the human immune response induced by repeated malaria infections to the *Plasmodium falciparum* antigen PF155/RESA. Int. Immunol. **3:**1043–1051.
55. **Wang, P., and E. Hilton.** 2001. Contribution of HLA alleles in the regulation of antibody production in Lyme disease. Front. Biosci. **6:**B10–B16.
56. **Yokoyama, W. M., F. Koning, P. J. Kehn, G. M. Pereira, G. Stingl, J. E. Coligan, and E. M. Shevach.** 1988. Characterization of a cell surface-expressed disulfide-linked dimer involved in murine T cell activation. J. Immunol. **141:**369–376.
57. **Yokoyama, W. M., S. R. Maxfield, and E. M. Shevach.** 1989. Very early (VEA) and very late (VLA) activation antigens have distinct functions in T lymphocyte activation. Immunol. Rev. **109:**153–176.
58. **Ziegler, S. F., F. Ramsdell, and M. R. Alderson.** 1994. The activation antigen CD69. Stem Cells **12:**456–465.
59. **Zivny, J., I. Kurane, C. O. Tacket, R. Edelman, and F. A. Ennis.** 1993. Dengue virus-specific, human CD4+ cytotoxic T lymphocytes generated in short-term culture. Viral Immunol. **6:**143–151.